

# Transition Metal-Based Spectrally Selective Coatings Using In-House Developed Spray System

Ajoy K. Saha, Laltu Chandra and Ambesh Dixit

**Abstract** The development of transition metal (Fe, Co, Ni, Mn) oxides based thin coatings is reported on stainless steel substrates for solar absorber applications. Absorber layers are synthesized using in-house developed spray system for metal–metal oxide composite coating structures. The optimized combinations of transition metal precursors are sprayed for thin film deposition. The post-spray heat treatment has been carried out to convert the transition metal precursor layers into spectrally selective absorber coatings showing metal–metal oxide composite structures. Three combinations of bi-transition metals Co–Mn, Co–Fe, and Co–Ni precursors are used to synthesize thin film structures. The thickness of these thin films structures is nearly 1  $\mu\text{m}$ . These spectrally selective coatings exhibit high absorptivity ( $\alpha \sim 0.9$ ) in 300–900 nm wavelength range and emissivity ( $\varepsilon \sim 0.18$ –0.44) in 2.5–25  $\mu\text{m}$  wavelength range. The extension of this work is focused on the development of a large-scale system, capable of fabricating spectrally selective coating on desired structures and optimization of annealing conditions, leading to the optimum solar thermal performance with high absorptivity ( $\alpha > 0.95$ ) and low emissivity ( $\varepsilon < 0.1$ ) in the desired wavelength ranges.

**Keywords** Solar · Energy · Coating · Spray · Metal · Oxides

---

A.K. Saha

Center for Solar Energy, Indian Institute of Technology Jodhpur,  
Old Residency Road, Ratanada, Jodhpur 342011, Rajasthan, India

L. Chandra

Department of Mechanical Engineering and Center for Solar Energy,  
Indian Institute of Technology Jodhpur, Jodhpur 342011, Rajasthan, India

A. Dixit (✉)

Department of Physics and Center for Solar Energy, Indian Institute of Technology Jodhpur,  
Jodhpur 342011, Rajasthan, India  
e-mail: ambesh@iitj.ac.in

## 1 Introduction

The utilization of abundant renewable solar energy is important to reduce the reliance on rapidly depleting fossil fuels. Concentrated solar thermal (CST) technologies are gaining attention, where solar energy is converted into thermal energy for possible applications including electricity generation [1]. CST technologies rely on the design and development of cost-effective solar absorber coatings. An efficient solar absorber coating should exhibit high absorptivity ( $\alpha > 0.9$ ) and low emissivity ( $<0.1$ ) characteristics over the desired wavelength and operating temperature range [1]. Several techniques are available, including spray, sputtering, electrochemical, and chemical vapor deposition (CVD) [2] for fabricating spectrally selective surfaces. Although physical and chemical vapor deposition techniques have been exploited for solar absorber films, their application is limited to small planar substrates. However, CST technologies require coatings to be developed for larger surfaces like pipes, curved surfaces and specific physical and chemical vapor deposition systems have to be developed for such real applications. In such cases, wet chemical techniques, such as spray and electrochemical techniques, may provide an alternative to fabricating such layered structures. Among the wet chemical techniques, sol-gel [3–5] based dip coating and electrochemical [6–8] routes have been investigated widely for spectrally selective coating applications. However, little literature is available on the spray technique [9, 10], especially for solar selective coatings. The spray pyrolysis technique has been used to fabricate black nickel [9] coatings on Al and galvanized iron substrates. Uma et al. [10] synthesized cobalt oxide-iron oxide coatings using similar techniques. However, considering the high flexibility and cost effectiveness of spray technique for solar absorber coating fabrication, the spray route needs to be designed and optimized extensively, for small and large surface coating applications. Here, we discuss the design and development of a semi-automated spray system, as explained schematically in Fig. 1, which can be used to fabricate the solar absorber coatings on any type of surfaces such as curved surfaces, tubes, pipes, and planar substrates. The system provides length, breadth, and height variability to optimize the quality of the thin films. In addition, the gas flow and precursors flow rates can be used as the control parameters to further improve the film quality and materials' composition for desired structural, optical, and solar thermal properties. Thus, the intended system may provide complete flexibility to engineer the design parameters for desired solar thermal properties and geometrical scalability for coatings on any desired surface. The initial work has focused to demonstrate the feasibility of this process on a smaller scale, where precursor solutions for coatings were sprayed on stainless steel (SS) substrates, 3 cm  $\times$  2 cm sizes, using a manually operated spray gun and sprayed structures were subjected to the heat treatment for creating the metal-metal oxide composite matrix for desired solar thermal properties.

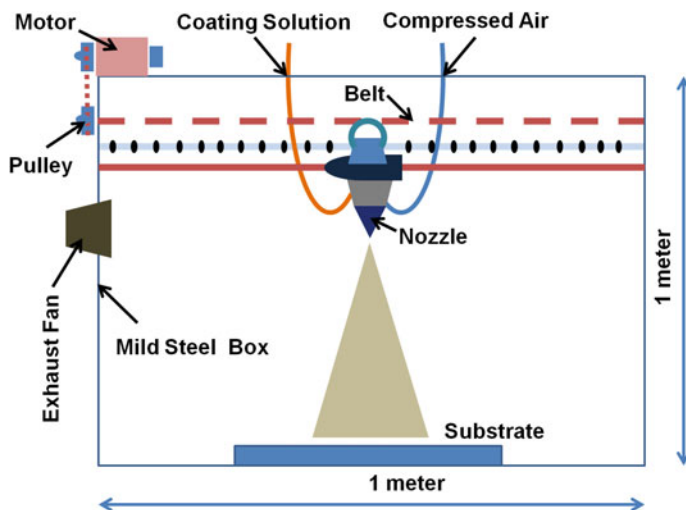


**Fig. 1** Schematic of semi-automatic spray coating setup, with legends explaining the respective components used in the system's development

## 2 Experiment

The spray coating setup consists of a 1 m × 1 m × 1 m stainless steel structural framework. The sides are covered by thin light MS steel plates for protecting the spillage of material during the spray process. This setup includes a motor (Nex Robotics, 170RPM 37DL), driven by L298 Motor Driver Kit and controlled by a microcontroller (Arduino Mega 2560 R3), belt, and pulley (Robokits, GT2 timing pulley 20 teeth, 6 mm width, 5 mm bore diameter) system, which is utilized for to and fro motion of the liquid spraying nozzle along the entire X-axis, as explained in Fig. 1. The system consists of (i) precursor line and (ii) gas line, as marked in Fig. 1. The flow rates of both, precursor and gas can be controlled independently to regulate the end flow rate across the nozzle and thus the film thickness during spray deposition. The base of the spray system has been used for holding substrates without and with a controlled heating assembly for desired processing temperature. The coating precursor solution is sprayed using compressed air, where the distance between substrate and spray nozzle can be adjusted for optimal spraying conditions. In another attempt, some samples were prepared by spraying solutions using a spray gun to test and optimize the precursors spraying conditions. The spray solution was prepared by dissolving transition metal (Ni, Co, Mn and Fe) salts in ethyl alcohol.

Ethanolamine was used as a chelating agent, while polyethylene glycol was added to obtain the optimum viscosity required for spraying the prepared solution. Stainless steel (SS) substrates were cut in sizes of 3 cm × 2 cm from larger plates. They were ground with 2000 grade grinding paper followed by washing with lime and salt. Subsequently, to remove oily contaminants, the ground substrates were

**Fig. 2** Optical photographs of spray coated thin films on SS substrates, using transition metals (Fe, Ni, Co and Mn) in ethyl alcohol, heat-treated at 100 °C for 1 h



treated with trichloroethylene at 80 °C for 5 min followed by acetone under similar conditions. The cleaned substrates were then dried by dabbing with disposable tissues. The substrates, thus prepared were mounted on a big steel plate by pasting them with paper tapes for deposition of desired precursors' thin films at room temperatures. The setup was arranged vertically inside a fume hood and then sprayed with the precursor solution using the spray gun. For good quality coating, the optimum spray distance was fixed at about 1 m from the substrates. The spraying was continued to and fro from one end to the other for several times, to achieve the desired thickness of the coated thin films. The coating thickness variation needs to be strictly monitored for optimum coating performance during the spray process using different control parameters such as nozzle to substrate distance, stepping speed, and controlled flow rates of precursor and gas. The optical photographs of the room temperature sprayed thin films are shown in Fig. 2. The structural and microstructural property evaluations of the synthesized materials were carried out using X-ray diffractometer (XRD) and scanning electron microscopic (SEM) measurements. The optical properties were investigated using UV–Vis and Fourier transform infrared (FTIR) spectrophotometers. The obtained measurements were used to estimate the room temperature solar thermal response of these film structures.

### 3 Results and Discussions

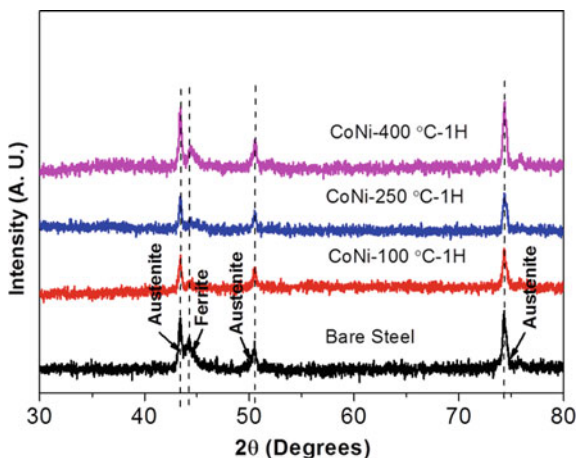
The transition metal (Fe, Ni, Co, Mn) salts in ethyl alcohol were used as precursors and sprayed on these cleaned stainless steel substrates to fabricate CoMn, CoFe, and CoNi thin film coatings. The different combination of bi-transition metal precursors produced different colored coatings.

The color of the as-prepared films produced using Co and Ni precursor salts was reddish, while those prepared from Co and Fe resulted in the greenish color. The color of the films containing Co and Mn was pink, as shown in Fig. 2. These as-prepared coatings were dried in air at room temperature for about an hour, followed by air drying in an oven at 100 °C for 1 h. The coated films retained their original color under such heating conditions up to 100 °C. These thin films spread uniformly over the substrate and exhibited good adhesive properties. These air dried coatings were further heated at 250 and 400 °C for 1 h each in open ambient conditions. The pristine color of these different colored coatings changed into the dark black after 250 °C and higher temperature treatment. This color change is due to the formation of transition metal oxides at higher temperatures, where band gap of transition metal oxide composites gave rise to the absorption and thus the dark black color of these annealed thin films. In contrast, the as-prepared thin films are colored because of intrinsic d-d electronic transitions in different transition metals, corresponding to different wavelengths. The structural evolution of these films has been investigated using XRD measurements with  $2\theta$  from 30° to 80° and the results are plotted in Fig. 3. The XRD spectrum of bare stainless steel substrate was also recorded and plotted in the bottom panel of Fig. 3, for comparison, and to distinguish the developed transition metal oxide structures on the SS substrate.

The XRD spectra of bare SS substrates exhibit austenite and ferrite phases, as indicated in the bottom panel of Fig. 3. The fabricated structures, annealed at different temperatures do not show any additional XRD peaks indicating that the transition metal oxide coatings are amorphous in nature. The surface microstructure and chemical compositions of these coatings were investigated using scanning electron microscopy and EDX measurements for heat-treated structures at 100, 250 and 400 °C and micrographs are shown in Fig. 4.

The bare SS substrate, shown in Fig. 4a suggests large cracks developed during the cleaning of the substrate with coarse abrasive paper. The surface micrographs of coatings heated at different temperatures are shown in Fig. 4b–d. The surface SEM

**Fig. 3** XRD spectra for CoNi bi-transition metal coatings on SS substrate after heating at 100, 250, and 400 °C for 1 h with bare SS substrate



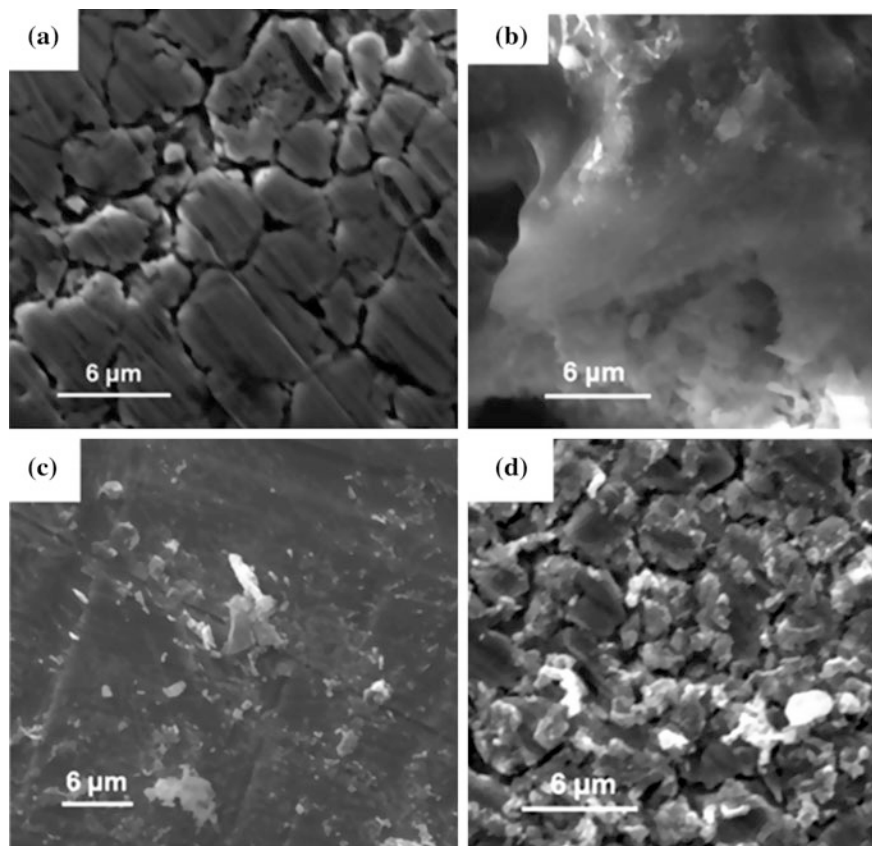


**Fig. 4** Scanning electron microscopic images of, **a** bare steel substrate, coatings containing Co and Mn after heating at **b** 100 °C, **c** 250 °C and **d** 400 °C for 1 h

image of 100 °C heat-treated sample, Fig. 4b, is floppy in nature indicating the presence of unburnt organic materials present in the spray precursor solutions. The surface of heat-treated sample at 250 °C, Fig. 4c, shows coating on SS along with the cracks, and granular coverage with larger grain boundaries. In contrast, a surface micrograph of heat-treated sample at 400 °C, Fig. 4d, shows a smooth surface, suggesting the formation of uniform film across the substrate. This is because of the interdiffusion of transition metal and oxygen to form uniform transition metal oxide—transition metal composite thin film uniformly across the substrate at higher temperature. The EDX elemental analysis results are summarized in Table 1 for these films, annealed at various temperatures, together with the chemical composition of the SS substrate.

The EDX spectrum of bare SS substrate indicates the presence of ~74 at% Fe, 9 at% Mn and 17 at% Cr elements. The thin films prepared using Co and Mn metal precursors and heated at 100 °C exhibit ~6.4 at% Co and 1.2 at% Mn respectively,

**Table 1** EDX analysis of films containing Co and Mn after annealing at **a** 100, **b** 250 and **c** 400 °C, relative to the bare stainless steel substrate

Coatings	SS with coating (at%)			Bare SS substrate	
	Element	100 °C	250 °C	400 °C	Element
C	57.4	–	–	C	–
O	29.1	20.1	38.0	O	–
Cr	1.2	12.4	8.4	Cr	17.1
Mn	1.2	7.4	7.0	Mn	8.9
Fe	4.1	56.0	38.4	Fe	74.1
Co	6.4	4.2	8.3	Co	–

with 57.4 at% C and ~29.1 at% oxygen, confirming the presence of precursor unburnt organic material in the sample. The SEM micrograph of the sample above also confirms the same, where floppy surface morphology has been observed because of unburnt organic contents in the coating. The presence of oxygen does not indicate the conversion of Co and Mn into transition metal oxides for 100 °C annealed samples, as their color remains intact, suggesting the presence of metallic transition metals in general. However, samples annealed at 250 °C showed the absence of C and reduction in oxygen atomic fraction and is ~20 at% only, substantiating the observed undecomposed organic precursors at 100 °C and partial conversion of transition metals into respective oxides. The oxygen atomic fraction enhanced up to 38 at% for 400 °C annealed samples, indicating the increase in transition metal oxide compositions against the unreacted metallic fraction in less temperature annealed samples. In addition to the Co and Mn elements, Fe and Cr are also observed for all samples, explaining the EDX elemental contribution from substrates. The carbon decomposed completely at higher annealing temperatures ~250 and 400 °C. This may be due to the lower decomposition temperatures of initially selected precursors or the content is lower than the detection limits of EDX, used in the present studies. The thicknesses of the coatings were determined from stepped SEM measurements, as illustrated in Fig. 5.

The thickness of these films is around ~1.15  $\mu\text{m}$  and that of SS substrates is ~0.1 mm, as marked in Fig. 5. The optical properties such as absorptivity and emissivity are measured using UV–Vis and Fourier Transform Infrared (FTIR) reflectance measurements in 300–900 nm and 2.5–25  $\mu\text{m}$  wavelength range, respectively. The measured absorptance values for all the samples, annealed at 400 °C are plotted in Fig. 6. We observed that the absorber films prepared from different transition metal precursors, and annealed at 400 °C, as explained in Fig. 6, exhibit  $\alpha$  nearly ~0.9, independent of transition metal precursor choice. However, the absorptivity  $\alpha$  values increase with annealing temperature, and the measured  $\alpha$  values are listed in Table 2.

These results also substantiate that  $\alpha$  is nearly independent of the transition metal precursor choice and values are constant for thin film coating structures annealed at the same temperatures. When compared with the  $\alpha$  value of bare SS, which is 0.41, those obtained for the coatings are found much higher, the absorption in coating

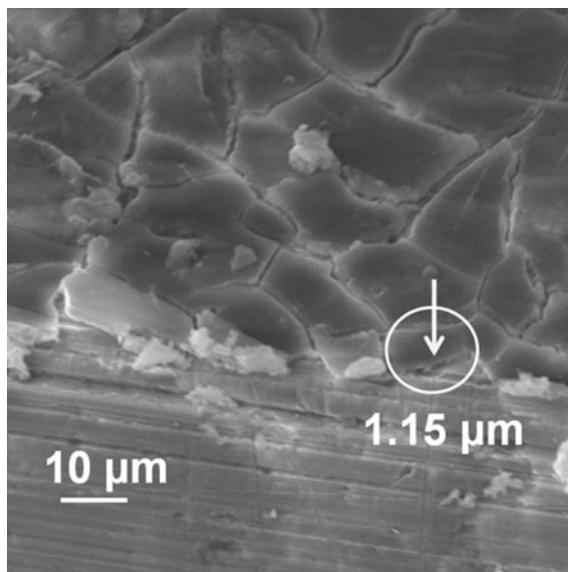


**Fig. 5** Scratched surface of a Co and Fe-containing film, heat treated at 250 °C, showing film thickness ~1.15 μm

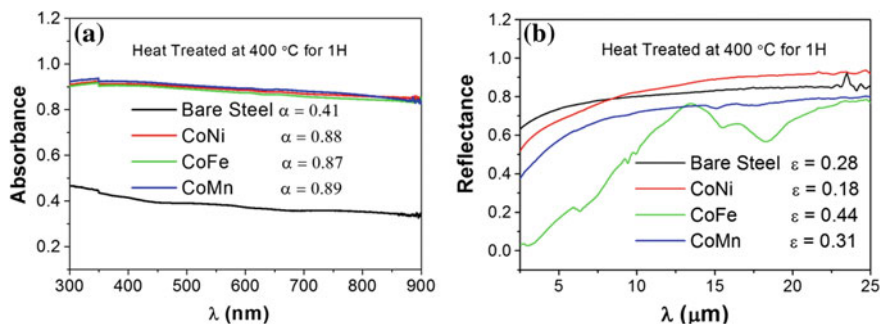


**Fig. 6** The absorbance (a) and reflectance (b) plots for the transition metal absorber layers against wavelengths, and SS substrate

**Table 2** Absorbance values for the transition metal oxide coatings when heated at 100, 250, and 400 °C

Coatings	$\alpha$		
	100 °C	250 °C	400 °C
CoNi	0.64	0.66	0.88
CoFe	0.64	0.74	0.87
CoMn	0.62	0.71	0.89



structures is mainly due to the metal–metal oxides composite structures, formed during controlled oxidation of transition metal precursors. The wavelength range of 300–900 nm is used in these measurements, due to the limitation of the UV–Vis spectrometer operating range.

The observed trend of large values in absorbance within the 300–900 nm regime, may continue till 2500 nm and the integrated absorbance may even be larger than those obtained for these samples. The measured emittance values are plotted in Fig. 5b. For bare SS substrate  $\varepsilon \sim 0.28$  and 400 °C annealed CoNi, CoFe, CoMn precursor based coating structures emissivity values are 0.18, 0.44, and 0.31, respectively. The observed  $\varepsilon$  values are higher than the desired values for spectrally selective coatings, used in solar thermal applications.

This may be due to the absence of the infrared reflecting layer between the substrate and transition metal coating structures. Similar observations of high  $\varepsilon$  values have also been observed in the case of without infrared reflecting layer for electrodeposited black chrome solar selective absorbers. In black chrome absorber layers, nickel infrared reflector plays an important role to reduce the emissivity  $\sim 0.1$  or less [11]. Additionally, the values of  $\varepsilon$  can be tailored further by optimizing the annealing conditions for these structures, causing the controlled oxidation of coated structures, leading to optimized metal–metal oxide based cermet structures, thus providing the desired  $\varepsilon$  values. The measured UV–Vis normal reflectance values are used to calculate the refractive index,  $n$  and extinction coefficient,  $k$  for the metal–metal oxide thin films in the 300–900 nm wavelength range using the following formulae:

$$n = \frac{100 + \sqrt{R}}{100 - \sqrt{R}}, \quad (1)$$

$$k = \frac{A\lambda}{4\pi} \quad (2)$$

where  $R$  is the measured reflectance and  $A$  is the absorption coefficient of the films. The measured results are summarized in Fig. 7. These measurements suggest that  $n$  for bi-transitional metal oxide films are nearly independent at higher wavelength and shows variation near lower wavelengths. The extinction coefficient  $k$  values for metal oxide films are much larger as compared to bare stainless steel substrate, suggesting the observed high absorbance in these metal–metal oxide thin films structure over the entire 300–900 nm wavelength range. The detailed compositional and elemental analysis will help in understanding the contribution of different components responsible for large extinction coefficient values. The extension of the present work is focused on the development of large-scale coating on specific surfaces and optimization of annealing conditions for desired values of absorptivity and emissivity of the fabricated structures.

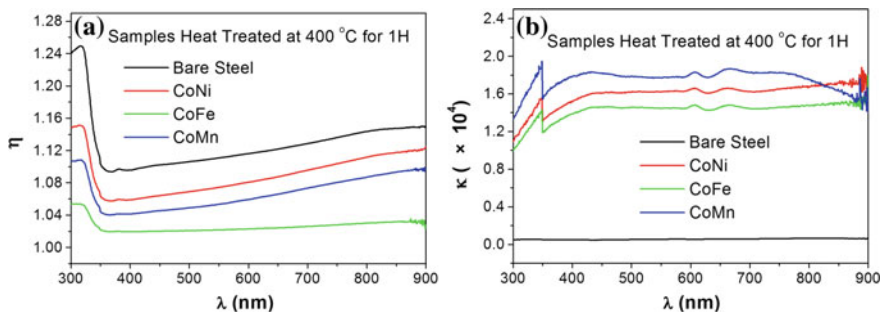


**Fig. 7** Plots of **a** refractive index,  $n$  and **b** extinction coefficient,  $\kappa$  of the films heated at 400 °C against respective wavelength  $\lambda$  in the 300–900 nm range. The abrupt jump at 350 nm in  $\kappa$  is because of the grating cross-over during measurements

## 4 Conclusion

We report the development of mixed transition metal oxide spectrally selective films on SS substrates for solar thermal applications using in-house developed spray coating system. The metal–metal oxide composite absorber layer coatings exhibit high absorptivity ( $\alpha \sim 0.9$ ) in 300–900 nm wavelength range. The thickness of these films is around 1  $\mu\text{m}$  and can be tailored as per requirement. The development of the large-scale system and integration of infrared reflecting layer are in progress to realize the spectrally selective coatings on the desired surface with optimal solar thermal performance such as high absorptivity ( $\alpha > 0.9$ ) and low emissivity ( $\varepsilon < 0.1$ ).

**Acknowledgements** Authors acknowledge financial assistance from Ministry of New and Renewable Energy (MNRE) through project #15/40/2010-11/ST. Author Ajoy K. Saha acknowledges Rajesh Kumar, Vinod Kumar, Gaurav Kumar, Rakesh Joshi, and Devaiah Soyam for their valuable suggestions and discussions during the work.

## References

1. N. Selvakumar, H.C. Barshilia, *Sol. Energy Mater. Sol. Cells* **98**, 1–23 (2012)
2. C.E. Kennedy, *Review of Mid-to High-Temperature Solar Selective Absorber Materials*. (National Renewable Energy Laboratory, Golden, Colorado, USA 2002), p. 1617
3. L. Kaluža, A. Šurca-Vuk, B. Orel, G. Dražič, P. Pelicon, *J. Sol-Gel. Sci. Technol.* **20**, 61 (2001)
4. M. Jolya, Y. Antonettia, M. Pythona, M.A. Gonzalez Lazoa, T. Gascoua, A. Hessler-Wyserb, J.-L. Scartezzinia, A. Schülera, *Energy Procedia* **57**, 487–496 (2014)
5. L. Kaluza, B. Orel, G. Drazic, M. Kohl, *Sol. Energy Mater. Sol. Cells* **70**, 187–201 (2001)
6. M.-L. Cantúa, A.M. Sabiob, A. Brustengac, P.G. Romeroa, *Sol. Energy Mater. Sol. Cells* **87** (1–4), 685–694 (2005)

7. M. Voinea, A. Duta, J. Optoelectron. Adv. Mater. **9**(5), 1454–1456 (2007)
8. G.E. McDonald, NASA Technical Memorandum TMX-71596, (1974)
9. M. Madhusudana, H.K. Sehgal, Appl. Energy **10**(1), 65–74 (1982)
10. C.S. Uma, L.K. Malhotra, K.L. Chopra, Bull. Mater. Sci. **8**(3), 385–389 (1986)
11. Y.A. Cengel, Heat and Mass Transfer: A Practical Approach, 3rd edn. (2008)